Eur Biophys J (2008) 37:121–129
DOI 10.1007/s00249-007-0184-9

ORIGINAL PAPER

Structure and elastic properties of tunneling nanotubes

Bruno Pontes · Nathan B. Viana · Loraine Campanati · Marcos Farina · Vivaldo Moura Neto · H. Moysés Nussenzveig

Received: 21 December 2006 / Revised: 27 April 2007 / Accepted: 7 May 2007 / Published online: 28 June 2007

Abstract We investigate properties of a reported new mechanism for cell–cell interactions, tunneling nanotubes (TNT's). TNT's mediate actin-based transfer of vesicles and organelles and they allow signal transmission between cells. The effects of lateral pulling with polystyrene beads trapped by optical tweezers on TNT's linking separate U-87 MG human glioblastoma cells in culture are described. This cell line was chosen for handling ease and possible pathology implications of TNT persistence in communication between cancerous cells. Observed nanotubes are shown to have the characteristic features of TNT's. We find that pulling induces two different types of TNT bifurcations. In one of them, termed V-Y bifurcation, the TNT is first distorted into a V-shaped form, following which a new branch emerges from the apex. In the other one, termed I-D bifurcation, the pulled TNT is bent into a curved arc of increasingly broader span. Curves showing the variation of pulling force with displacement are obtained. Results yield information on TNT structure and elastic properties.

Keywords Tunneling nanotubes · Structure · Elastic properties · Optical tweezers · Tethers · Bifurcations

Electronic supplementary material The online version of this article (doi:10.1007/s00249-007-0184-9) contains supplementary material, which is available to authorized users.

B. Pontes · N. B. Viana · L. Campanati · M. Farina · V. M. Neto · H. M. Nussenzveig (✉)
LPO-COPEA, Instituto de Ciências Biomédicas,
Universidade Federal do Rio de Janeiro,
Rio de Janeiro 21941-590, Brazil
e-mail: moyses@if.ufrj.br

N. B. Viana · H. M. Nussenzveig
Instituto de Física, Universidade Federal do Rio de Janeiro,
Caixa Postal 68528, Rio de Janeiro 21941-972, Brazil

Introduction

Cell–cell interactions are a vital requirement for the organization of tissues and cellular development. They occur early, signaling biochemical exchanges responsible for cell differentiation, proliferation, and/or migration. Cell–cell contacts via extracellular matrix or interaction by secretion of growth factors have been considered in the study of development. Here, we analyze properties of a proposed new system of communication between cells.

It has recently been reported (Rustom et al. 2004) that interconnection channels among cells, referred to as tunneling nanotubes (TNT), mediate selective, actin-based transfer of membrane vesicles and organelles among them. It was conjectured that they represent a new form of cell-to-cell communication, possibly requiring revision of basic principles of cell theory (Baluska et al. 2004). Similar structures, termed cytonemes, had previously been observed in *Drosophila* morphogenesis (Ramírez-Weber and Kornberg 1999) and they have also been related to actin-based signal transduction (Hsiung et al. 2005). TNT networks connecting dendritic cells have been shown as well to mediate intercellular signal transmission (Watkins and Salter 2005).

As characterized by Rustom et al. (2004), TNT's, observed *in vitro*, have the following characteristic features:

(a) typical radii of 25–100 nm;
(b) lengths of up to several cell diameters;
(c) tendency to form straight connections between cells;
(d) they contain F-actin (but not microtubules);
(e) they allow selective transfer of molecules and vesicles between cells;
(f) they are extended above the substrate, not attached to it;

(g) they are very sensitive to light excitation and mechanical stress, which tends to result in rupture;
(h) they may be generated by formation of filopodia-like cell protrusions.

Besides this de novo formation by actin-driven cell protrusion extending from one cell to another one (Rustom et al. 2004), TNT's can also be formed by an alternative mechanism, through separation of two initially linked cells, as observed upon disassembly of an immunological synapse (Önfelt et al. 2004). However, the detailed structure and elastic properties of TNT's remain unknown, motivating the present investigation.

Filopodia have been known for several decades (Gustafson and Wolpert 1961). They are found at the leading edge of motile cells and at the tip of the growth cone in migrating axons (Kater and Rehder 1995; for a brief review, see Wood and Martin 2002). Thin filopodia have radii of 100–200 nm, and they may also extend for tens of μm. They contain bundles of F-actin, and their formation and structure have been investigated (Pollard et al. 2000; Svitkina et al. 2003; Mogilner and Rubinstein 2005; Vignjevic et al. 2006).

In contrast with the dendritic nucleation of actin branches at the leading edge of cells, with their characteristic 70° angle about the axis, filopodia contain tightly packed bundles of actin filaments and they protrude from ''roots'' within the surrounding dendritic network behind the cell edge.

Filopodia play roles in locomotion, as sensors in navigation, in cell–cell adhesion, in signaling between cells, and for exerting forces, among others. There is also directed transport of receptors along filopodia (Lidke et al. 2005). Thus, while filopodia as transient short and thicker protrusions from single cells clearly differ from TNT's, distinctions between TNT's and long thin filopodia connecting cells are rather hazy: they share several features. Cells in culture are often surrounded by tubular extensions that can also be remnants of filopodia employed for adhesion and/or locomotion, or of incomplete cytokinesis (Rorth 2003).

A method often employed to determine membrane structure and elastic properties, both for cells and for artificial vesicles, is tether pulling (Bo and Waugh 1989; Dai and Sheetz 1995; Hochmuth et al. 1996; Dai and Sheetz 1999; Raucher and Sheetz 1999). In particular, this has been done by attaching a bead to the membrane and pulling on it with optical tweezers (OT) (Dai and Sheetz 1995; Li et al. 2002). Theoretical models of tether formation by direct pulling from cells have been proposed (Powers et al. 2002; Derényi et al. 2002).

When tethers are directly pulled from membranes by OT's, the tweezer force is exerted axially, i.e., parallel to the tether axis. In contrast with TNT's and filopodia, such tethers do not contain actin: they are hollow cylindrical pure membrane tubes (Dai et al. 1998). However, in order to form them, the membrane-cytoskeleton links must be ruptured. This affects the initial rise in the force-versus-displacement curve: the peak value required for separation depends on the strength of these links.

Once separation has been achieved, a drop to a lower value may be observed (Li et al. 2002), followed by a steady-state elongation regime in which tether length increases at constant force. The interpretation and magnitude of the drop have been related to the existence of a finite attachment area between the bead and the cell membrane, forming a patch: the drop magnitude (force overshoot) increases linearly with the patch radius (Koster et al. 2005). The steady-state elongation plateau has been attributed (Raucher and Sheetz 1999; Sheetz 2001) to the existence of a cell membrane reservoir from which extra membrane can be drawn. When this reservoir is exhausted, a steep rise in force is observed.

An additional parameter that needs to be taken into account is the velocity of tether extraction. As this velocity increases, extra force needs to be exerted, owing to effective viscosity arising from relative slip. Adhesion to the substrate can also play a role (Smith et al. 2004).

The aim of the present work is to investigate the structure and elastic properties of tunneling nanotubes connecting cells. In particular, in view of the reported fragility of TNT's, we set out to exert stress on them and measure their response.

We start from already preexisting TNT's, connecting different cells, so that the OT force on them is exerted laterally (through attached microspheres), rather than axially. In contrast with previously investigated tethers, they are not formed by pure membrane: they contain F-actin, as is characteristic of TNT's and filopodia.

Cell typical dimensions are appreciably larger than those of microspheres, so that beads tend to become attached to a cell by a patch of sizable area. In contrast, lateral attachment of a micron-sized microsphere to a cylindrical nanotube of much smaller radius may be regarded as a point contact, implying a much smaller attachment probability. In our experiments, this resulted in a smaller proportion of successful attachments.

Contrary to our initial expectation, based on the reported fragility of TNT's, that lateral tension would induce rupture, we found instead, as reported below, that it led to TNT bifurcations. To our knowledge, there are no prior investigations of lateral pulling effects on TNT's, and the results should yield relevant information about their structure and elastic properties.

Materials and methods

Cell culture

Human glioblastoma cell line U-87 MG was cultured in Dulbecco's modified Eagle's medium (DMEM-F12) containing L-glutamine, 10% fetal bovine serum, and 1% penicillin/streptomycin. Cells were maintained at 37°C in 5% CO_2. For optical and electron microscopy and OT experiments, cells were harvested with trypsin/EDTA and plated on a 10 × 10 mm glass coverslip (MatTek corporation) placed within a special 35 mm Petri dish, on the day before the experiments. Cell concentration was 2×10^5 cells/ml and 1 μl of uncoated polystyrene beads (3.04 μm diameter SIGMA) in 10% water solution was added to 2 ml of cell culture medium. All OT experiments, except for those involving vesicle transfer, were performed in a homemade CO_2 chamber adapted to the microscope, maintaining optimal culture conditions. For direct tether pulling from cell membrane, sterile coverslips were employed. For experiments with TNT bifurcations, coverslips were washed with detergent, rinsed with distilled water and UV sterilized. F-actin labeling was performed by staining with phaloidin-FITC.

Optical microscopy

We employed an inverted microscope (Eclipse TE300 Nikon) equipped with Plan APO 100 × 1.4 NA DIC H and Plan APO 60 × 1.4 NA DIC H objectives and with the temperature/CO_2 control chamber attached. For the OT experiments, images were collected by a CCD camera (Hamamatsu model C2400) and digitized by a SCION frame grabber. Fluorescence images were taken by a Cool Snap Pro Color Roper Scientific CCD camera that digitizes them directly to the computer, and were captured employing ImagePro Plus (© Media Cybernetics, Inc.). Image analysis was performed with ImageJ (http://rsb.info.nih.gov/ij), and data analysis with Kaleidagraph (© Synergy Software).

Optical tweezers

The OT setup employed the above-described Eclipse Nikon TE300 inverted microscope. The trapping laser was a Nd-YAG (1064 nm wavelength, Quantronix) laser, with maximum power of 3 W. The laser beam was expanded to an intensity profile with a halfwidth of 2.3 ± 10% mm at the back focal plane of the objective lenses. Force calibration of the trap was performed by comparison with fluid drag force, employing Faxen's correction to the Stokes law (Neuman and Block 2004).

$$F = 6\pi\eta a v \left[1 - \frac{9}{16}\left(\frac{a}{h}\right) + \frac{1}{8}\left(\frac{a}{h}\right)^3 - \frac{45}{256}\left(\frac{a}{h}\right)^4 - \frac{1}{16}\left(\frac{a}{h}\right)^5\right]^{-1}, \quad (1)$$

where F is the force, η is the fluid viscosity, a is the bead radius, v is the fluid velocity and h is the height of the bead center relative to the coverslip, determined as explained in Viana et al. (2006b). For water at 20°C, η = 1.005 cp (Lemmon et al. 2005). Measurements were performed at 3 μm < h < 12 μm. Attachment of the beads at these heights ensured that the TNT's extended above the substrate, and were not attached to it [feature (f), ''Introduction'' section].

The velocity v of the motorized stage of the microscope was monitored by a Prior controller, connected to the computer via the serial port, and the trapped bead equilibrium position as a function of stage velocity was measured. Bead displacement was obtained by analyzing the bead image with ImageJ software and identifying the position of its center of mass.

Equating the Stokes force with the trapping force, we get the trap stiffness. We use the dual-objective method to measure the power transmitted by the objective (Viana et al. 2006a) and we control trap stiffness by controlling the power at the objective entrance. With this procedure we get an uncertainty of 10% in force measurements. Further details on OT calibration are provided in Viana et al. (2006b).

Scanning electron microscopy

U-87 MG cells were seeded on special Petri dishes, as described in the ''Cell culture'' subsection, and after 24 h, fixed with 2.5% glutaraldehyde and 4.0% paraformaldehyde in 0.1 M cacodylate buffer (pH 7.4) overnight. After rinsing in the same buffer, the cells were post-fixed in OsO4 1% and 1.25% FeCNK for 40 min, rinsed again and dehydrated in an ethanol series. After removing the coverslip from the Petri dish, the samples were critical-point dried using a BAL-TEC CPD 030 Critical Point Drier and the coverslips mounted on specimen stubs.

The samples were then gold sputtered using a BAL-TEC SCD 050 Sputter Coater and observed in the Jeol Sem 5310. Image acquisition was made using Jeol SemAfore 3.0 acquisition system.

Field emission electron microscopy

In order to observe the cells cytoskeleton, we made use of membrane extraction techniques and the samples were observed in the field emission scanning electron microscope (Sant'Anna et al. 2005). Cells attached to glass coverslips were extracted using 1% Nonidet P-40 in 0.1 M

PHEM buffer (60 mM 1.4 piperazine diethylsulfonic acid (PIPES), 25 mM N-2-hydroxyethylpiperazine Nl-2-ethanesulfonic acid (HEPES), 10 mM EGTA, and 2 mM $MgC1_2$; Sant'Anna et al. 2005), pH 7.2, twice, for 1 h at 37°C. They were then washed in 0.1 M PHEM buffer and fixed in 2.0% glutaraldehyde in PHEM buffer for 30 min at room temperature. After washing, the cells were dehydrated using an ethanol series (50, 70, 90 and 100%) and were critical point dried and gold sputtered as described for routine scanning electron microscopy. Observation was done in a Jeol JEOL JSM-6340 FESEM.

Results

Direct tether extraction

Direct tether extraction is an important source of information about the elastic properties of cell plasma membranes (Titushkin and Cho 2006). Since such information should be valuable for theoretical modeling of our TNT observations, we undertook to first employ the OT setup for direct tether extraction from the cell line under investigation.

For this purpose, a polystyrene bead with 3.04 ± 0.02 μm diameter trapped by the OT was held for a few seconds on the cell surface and then pulled out at a constant velocity of 0.071 ± 0.005 μm/s by displacing the microscope stage, with digital recording of bead displacement.

Image analysis yielded the position of the bead center of mass as a function of time, and from the OT calibration (Viana et al. 2006b) we determined the corresponding variation of the force exerted on the tether.

A typical membrane tether (representative of about 10 observations) extracted by this procedure is shown in Fig. 1a, and the corresponding force × displacement curve is shown in Fig. 1b. The result is similar to that obtained with tether extraction from hair cells (Li et al. 2002; Fig. 8): an initial tether formation force rise is followed by a drop to a steady-state plateau. The significance of these results will be discussed in the ''Conclusion'' section.

TNT features

A typical U-87 MG cell culture kept for 24 h within the CO_2 chamber is shown in Fig. 2. In order to identify the nanotubes linking different cells that are seen in this figure as TNT's, we have checked that they have the characteristic features listed in the ''Introduction'' section:

Radius

Figure 3 shows scanning electron microscopy images of several nanotubes, as well as measurements of the grey-level distribution in the transverse section of one nanotube. Experimental points are fitted to a Gaussian

$$G(x) = G_M \exp\left(-\frac{x^2}{2R^2}\right) \quad (2)$$

to define the tube radius R. From the analysis of 11 different nanotubes, we found for the average radius the value

$$<R> = (48 \pm 6)\,\text{nm} \quad (3)$$

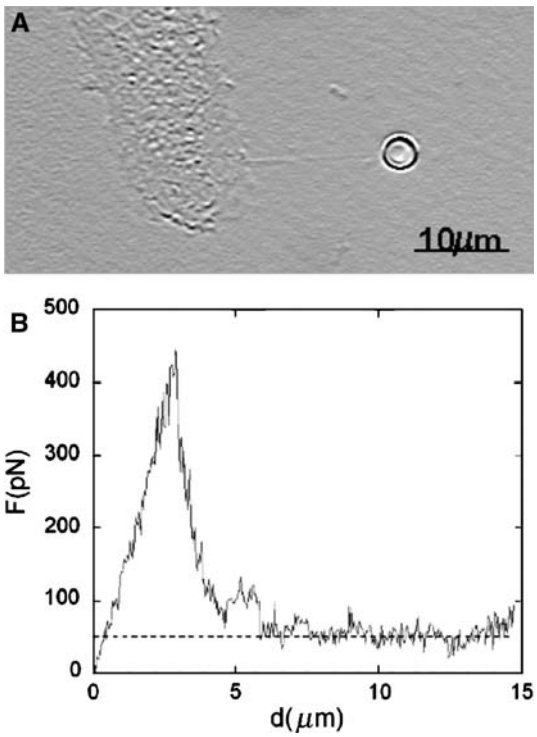

Fig. 1 Direct tether extraction from cell. **a** Membrane tether extracted from U-87 MG cell (Plan APO 100 × 1.4 NA DIC H objective; image processed with ImageJ Shadow North filter). **b** Force versus microscope stage displacement (velocity 0.071 μm/s). Dashed line is plateau average

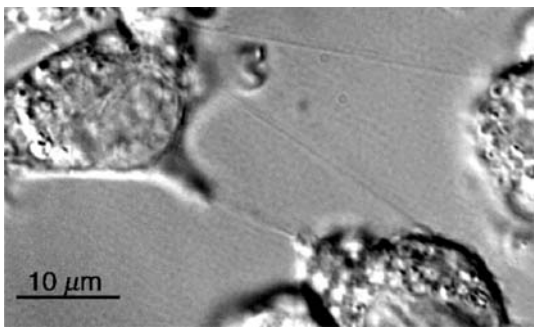

Fig. 2 U-87 cell culture showing TNT links. (Plan APO 100 × 1.4 NA DIC H objective)

This is well within the typical range of 25–100 nm.

Lengths

Figure 2, as well as other images below, shows typical nanotube lengths of tens of μm, again consistent with TNT's.

Straightness

This feature is also apparent in Fig. 2 and other images below.

F-actin content and absence of tubulin

To test for the presence of actin within the nanotubes, cultures were stained with phaloidin-FITC. Figure 4 shows results for a typical culture, Fig. 4a is a regular DIC image, while Fig. 4b is a fluorescence image of the same field, obtained by switching the system to the fluorescence mode. All observed nanotubes, like those shown, contain actin. Immunofluorescence tests for the presence of tubulin (not shown) gave negative results.

As a further check, cultures were treated with detergent to wash out cell membranes, and observed by field emission electron microscopy, as described above. Typical results, shown in Fig. 5, clearly reveal the F-actin filled structure of TNT's. They also indicate that TNT implantation inside cells looks very similar to that of filopodia (Pollard et al. 2000; Svitkina et al. 2003; Mogilner and Rubinstein 2005; Vignjevic et al. 2006), consistent with filopodial-like origin of TNT's (Rustom et al. 2004).

Vesicle transfer

Movie M1 (Supplementary material) shows transfer of a vesicle along a TNT linking U-87 MG cells cultured under stress conditions (no CO_2). Vesicle transfer was never observed under optimal culture conditions. Rustom et al. (2004) verified the transfer of organelles and membrane proteins through TNT's, but investigation of transferred contents is outside the present paper's main focus.

Extension above substrate

As remarked in ''Optical tweezers'' subsection, bead attachment to nanotubes in all experiments was performed at heights > 3 μm above the coverslip, ensuring that the nanotubes are extended above the substrate.

Sensitivity to stress

Mechanical stress during preparation for electron microscopy led to rupture of several nanotubes, as may be seen in Figs. 3 and 5 (cf. Rustom et al. 2004).

Formation

Movie M2 (Supplementary material) shows TNT formation through separation of two initially linked cells, similar to (Önfelt et al. 2004). We did not observe TNT generation by formation of filopodia-like cell protrusions as reported in (Rustom et al. 2004).

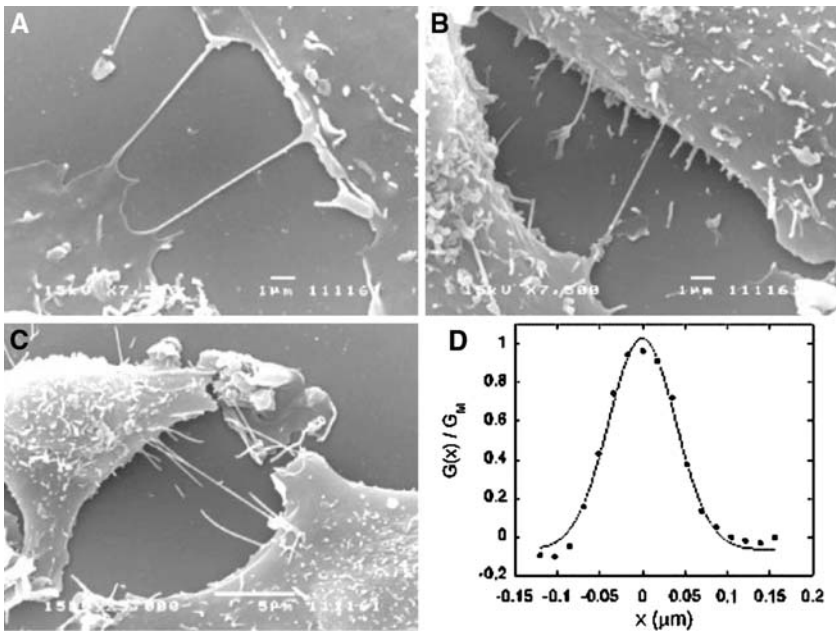

Fig. 3 Scanning electron microscopy images of TNT's. **a–c** Appearance of the nanotubes from different regions of U-87 cell culture. **d** Gaussian fit to grey-level distribution of one nanotube

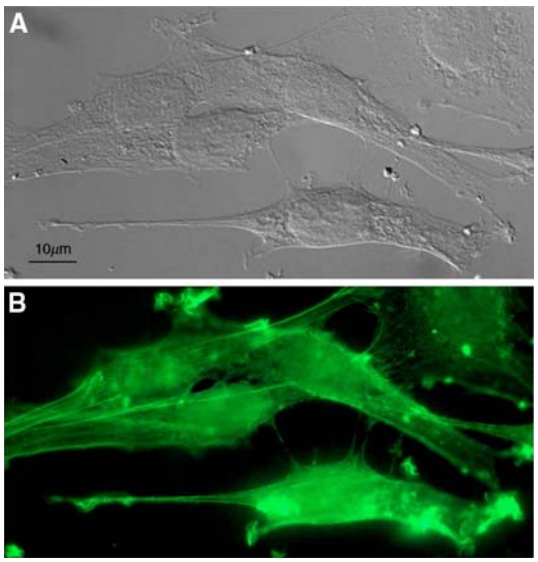

Fig. 4 Mapping of F-actin in U-87 MG cells. **a** DIC image of phaloidin-FITC-stained U-87 MG cells. **b** Fluorescent image of same field. Note that the nanotubular structures are stained with the fluorescent dye (color online)

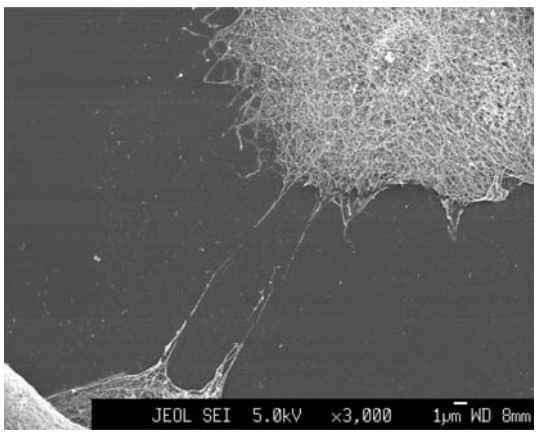

Fig. 5 Field emission electron microscopy image of U-87 MG cells. Nanotube breaks are presumed to arise from stress in sample preparation

V-Y bifurcation

For sideways pulling on a nanotube, an uncoated polystyrene bead with 3.04 ± 0.02 μm diameter, trapped by the OT, was held for several minutes (this was necessary for attachment) on the nanotube and then pulled out perpendicular to the nanotube, at a constant velocity of 0.071 μm/s, by displacing the microscope stage, while digitally recording the bead displacement. Image analysis yielded the position of the bead center of mass as a function of time, and from the OT calibration we determined the corresponding variation of the force exerted on the nanotube.

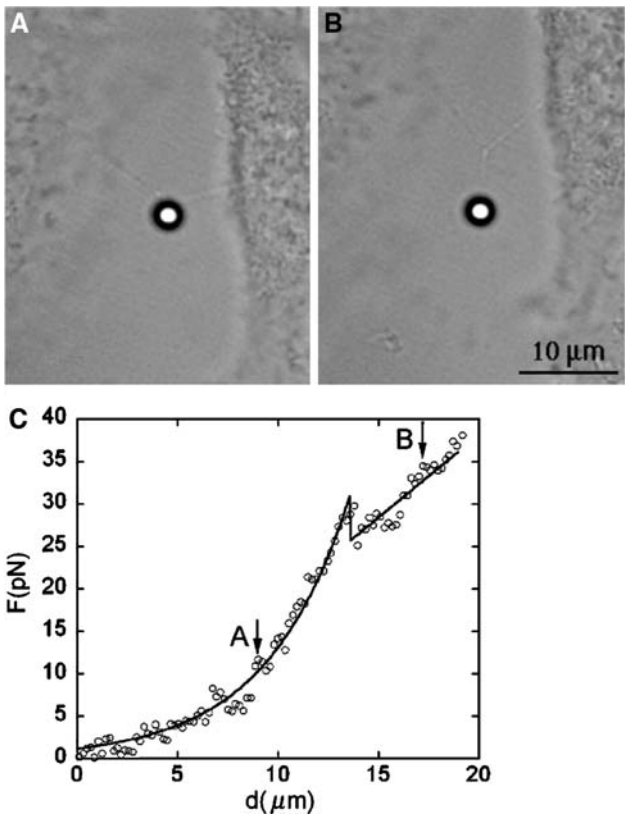

Fig. 6 V-Y bifurcation. **a** Before bifurcation. **b** After bifurcation. **c** Corresponding force versus microscope stage displacement (velocity 0.071 μm/s). Circles are experimental points. Curve drawn to guide the eye. Points corresponding to images **a** and **b** are marked by arrows. Bifurcation position coincides with the dip in the curve

The very small velocity of data point acquisition should have allowed local equilibrium to be established, so that the measured value of the force is taken to be the steady one. Achieving contact and production of lateral force was found to be difficult, as expected (see ''Introduction'' section), requiring many repeated efforts. Bead coating with laminin, an extracelular matrix glycoprotein, produced no improvement. Thus, successful observations are few.

Typical results of one kind of bifurcation, representative of four observations, are shown in Fig. 6 and Movie M3 (Supplementary material). Initially, as shown in Fig. 6a, the TNT was bent into a V shape, with the bead at the apex. As the OT force increased, instead of rupturing, a new branch emerged, yielding a Y shape. In five other observations (not included), the same characteristic nonlinear ascending force rise was seen, but bead release from the trap occurred before reaching the bifurcation.

We call this a V-Y bifurcation. The emergence of a new branch coincides with the dip in the force × displacement curve (Fig. 6c and Movie M3). Near this point, typical angles between adjacent branches are close to 120°.

A similar, and similarly named, bifurcation was previously observed in endoplasmic reticulum (ER) and Golgi nanotubular networks in vitro, by lateral pulling on a network nanotube through an OT-trapped bead (Upadhyaya and Sheetz 2004, Fig. 3). The triple point at the Y also relaxed to 120° angles. Spontaneously branched TNT's have also been observed, both in cultured PC12 cells (Rustom et al. 2004, Fig. 1c) and in a 3-way junction connecting three murine macrophage cells, again at 120° angles (Önfelt et al. 2004, Fig. 1c). Similar 3-way junctions with the same geometry are found in artificial liposome networks (Karlsson et al. 2001, 2002).

I-D bifurcation

Typical results of a different kind of bifurcation, representative of four observations, are shown in Fig. 7 and Movie M4 (Supplementary material). In this case, the initially straight TNT is bent into a curved arc, with a progressively broadening span as the force increases, producing a D-shaped structure. We call this an I-D bifurcation. Experimental points (Fig. 7b), in contrast with Fig. 6c, were taken at fixed d intervals of 1 μm, with rapid (~ 0.1 s) stage displacements followed by ~ 1 s waiting times.

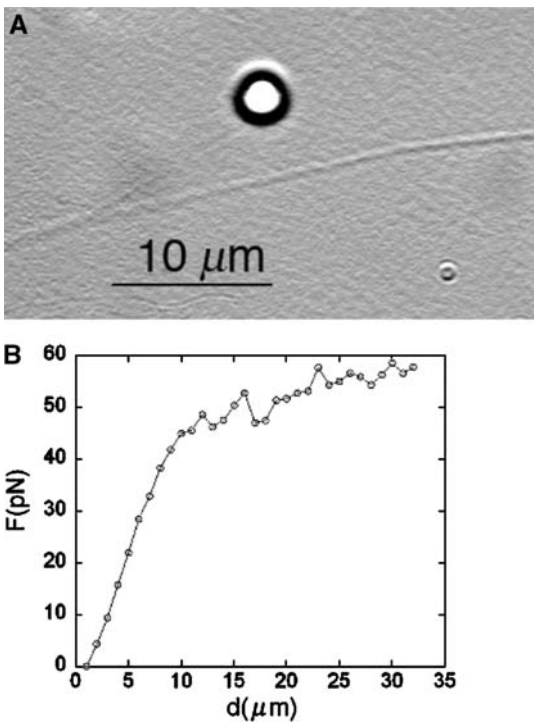

Fig. 7 I-D bifurcation. **a** After bifurcation. **b** Corresponding force versus microscope stage displacement (average velocity 1 μm/s). Circles are experimental points. Curve drawn to guide the eye

Discussion

We have investigated the properties of a new system of intercellular communication, tunneling nanotubes. We have used a tumoral cell line, and the observation of TNT linkages suggests that cell–cell information exchange is preserved even after malignant conversion, when cells are isolated from tissues. We have employed OT manipulation both for direct tether extraction from cells and for lateral pulling on TNT's. What can we infer from observed results about the structure and properties of TNT's?

If we interpret Fig. 1b by analogy with Fig. 8 in Li et al. (2002), which shows OT force as a function of time for tethers from outer hair cells, the tether formation force by direct pulling from the cell membrane is of the order of 400 pN, and the steady-state force is of the order of 50 pN.

The large value of the tether formation force suggests a strong membrane-cytoskeleton adhesion force in U-87 MG cells, although cell adhesion to the substrate can also play a significant role (Smith et al. 2004). Indeed, we found that use of new, sterile plates was essential to allow tether extraction.

The large ratio of formation force to steady-state force may be interpreted in terms of a force barrier for membrane tube formation, arising from a finite attachment area initially linking the bead to the cell membrane (Koster et al. 2005).

The steady-state force F is usually related to the tether radius R, membrane bending rigidity B and effective surface tension T by the relations (Hochmuth et al. 1996)

$$F = 4\pi RT = 2\pi B/R = 2\pi\sqrt{2BT} \tag{4}$$

It is difficult to perform a direct measurement of tether radius. If we assume that R is of the order of the average TNT radius Eq. (3) found in a typical culture, $R \sim 50$ nm, we find that $T \sim 0.08$ pN/nm, $B \sim 4 \times 10^{-19}$ N m, which are not unreasonable values (Mogilner and Rubinstein 2005; Derényi et al. 2002; Bukman et al. 1996). However, the value of R is an assumption.

We now turn to the results for the V-Y bifurcation. The nonlinear ascending portion of the curve in Fig. 6C is associated with the force exerted for bending the TNT into a V shape. Interestingly, the dip at the bifurcation point represents a force reduction of the order of 10%, consistent with an overshoot force 13% higher than steady state, as found for a point pulling force on membrane (Derényi et al. 2002; Koster et al. 2005). Attachment of the bead to a thin cylindrical nanotube should be closer to a point contact than direct attachment to the (much larger) cell. This would also explain why it is difficult to establish a tight enough contact with a nanotube to begin deforming it into a V shape (a much longer contact time is required).

The approximately linearly rising portion of the curve beyond the bifurcation point may signal the absence of a membrane reservoir in this situation (Raucher and Sheetz 1999), in contrast with the situation found in Golgi and ER nanotubular networks (Upadhyaya and Sheetz 2004), where a virtually unlimited supply is available.

Let us assume (Upadhyaya and Sheetz 2004) that the radius of the new branch forming the Y is the same as the nanotube radius, $R \sim 50$ nm. Then, if we take for the force the value just beyond the bifurcation, $F \sim 30$ pN, Eq.(4) yields the values $T \sim 0.05$ pN/nm, $B \sim 2.4 \times 10^{-19}$ N m, which are quite reasonable. Again, of course, to go beyond these order-of-magnitude estimates, one needs a theoretical model of the V-Y bifurcation; existing tether formation models do not take into account the change in topology.

The 120° angle configuration, formed also by self-organization in artificial liposome networks (Karlsson et al. 2001, 2002), corresponds to path (and surface free energy) minimization.

Finally, let us consider the I-D bifurcation. Figure 6a and Movie M4 indicate that, rather than a single TNT, two TNT's are involved, possibly even entwined with each other. By shifting the field of view and following the image, it was confirmed in one example of this bifurcation that there was indeed a double nanotube. Formation of multiple membrane tethers has been theoretically discussed (Derényi et al. 2002) and experimentally observed (Sun et al. 2005), although under very different conditions from those prevailing here. If two adhered TNT's are involved, the curve in Fig. 6b includes, besides TNT bending, the force needed to gradually separate one TNT from the other one.

Conclusion

We have performed, to our knowledge for the first time, OT lateral pulling experiments on TNT's linking different cells in vitro, obtaining data on force versus displacement. We have observed two different kinds of bifurcations. One of them, termed V-Y bifurcation, had previously been seen (Upadhyaya and Sheetz 2004) in endoplasmic reticulum (ER) and Golgi nanotubular networks in vitro, a quite different situation, since it occurs with hollow, pure membrane nanotubes (not TNT's) and the interconnected network supplies a virtually unbounded membrane reservoir. The other kind of observed bifurcation, termed I-D bifurcation, is possibly related to separation of one nanotube from a doublet.

It is interesting to note that the elastic properties of TNT's do not appear to be fundamentally different from those of pure membrane (hollow) nanotubes, in spite of their actin content. This suggests that their internal structure may be comparable to that of the thin filopodia from which they can originate, containing thin bundles of axially oriented F-actin, not very strongly attached to the TNT membrane.

Order-of-magnitude estimates of TNT bending rigidity and effective surface tension were given, based on assumptions about nanotube radius and on a widely employed tether growth model. Validation of such elastic parameters will require direct radius measurement of the specific nanotube observed as well as formulation of a detailed theoretical model of TNT bifurcations.

Focus of the present work was on the mechanical and structural properties of TNT's. Further investigations on their functions, comparisons with other cell types and possible pathology implications are under way.

Acknowledgments This work was supported by the Brazilian agencies Conselho Nacional de Desenvolvimento Científico e Tecnológico (CNPq), Coordenação de Aperfeiçoamento de Pessoal de Nível Superior (CAPES), Instituto do Milênio de Nanociências, Instituto do Milênio de Avanço Global e Integrado da Matemática Brasileira, Fundação de Amparo à Pesquisa do Rio de Janeiro (FAPERJ) and Fundação Universitária José Bonifácio (FUJB). We thank Jair Koiller and Gerusa Alexsandra de Araújo for helpful discussions.

References

Baluska F, Volkmann D, Barlow PW (2004) Eukaryotic cells and their *cell bodies*: Cell theory revised. Ann Bot 94:9–32

Bo L, Waugh RE (1989) Determination of bilayer membrane bending stiffness by tether formation from giant, thin-walled vesicles. Biophys J 66:509–517

Bukman DJ, Yao JH, Wortis M (1996) Stability of cylindrical vesicles under axial tension. Phys Rev E 54:5463–5468

Dai J, Sheetz MP (1995) Mechanical properties of neuronal growth cone membrane studied by tether formation with laser optical tweezers. Biophys J 68:988–996

Dai J, Sheetz MP (1999) Membrane tether formation from blebbing cells. Biophys J 77:3363–3370

Dai J, Sheetz MP, Wan X, Morris CE (1998) Membrane tension in swelling and shrinking molluscan neurons. J Neurosci 18:6681–6692

Derényi I, Jülicher F, Prost J (2002) Formation and interaction of membrane tubes. Phys Rev Lett 88:238101 1–238101 4

Gustafson T, Wolpert L (1961) Studies on the cellular basis of morphogenesis in the sea urchin embryo: directed movements of primary mesenchime cells in normal and vegetalized larvae. Exp Cell Res 24:64–79

Hochmuth RM, Shao JY, Dai J, Sheetz MP (1996) Deformation and flow of membrane into tethers extracted from neuronal growth cones. Biophys J 70:356–369

Hodneland E, Lundervold A, Gurke S, Tai X-C, Rustom A, Gerdes H-H (2006) Automated detection of tunneling nanotubes in 3d images. Cytometry A 69:961–972

Hsiung F, Ramírez-Weber F-A, Iwaki DD, Kornberg TB (2005) Dependence of *drosophila* wing imaginal disc cytonemes on decapentaplegic. Nature 437:560–563

Karlsson A, Karlsson R, Karlsson M, Cans A-S, Strömberg A, Ryttsén F, Orwar O (2001) Networks of nanotubes and containers. Nature 409:150–152

Karlsson M, Sott K, Davidson M, Cans A-S, Linderholm P, Chiu D, Orwar O (2002) Formation of geometrically complex lipid nanotube-vesicle networks of higher-order topologies. Proc Natl Acad Sci USA 99:11573–11578

Kater SB, Rehder V (1995) The sensory-motor role of growth cone filopodia. Curr Opin Neurobiol 5:68–74

Koster G, Cacciuto A, Derényi I, Frenkel D, Dogterom M (2005) Force barriers for membrane tube formation. Phys Rev Lett 94:068101–068104

Lemmon EW, McLinden MO, Friend DG (2005) Thermophysical properties of fluid systems. In: Linstrom PJ, Mallard WG (Eds) NIST chemistry WebBook. National Institute of Standards and Technology, Gaithersburg

Li Z, Anvari B, Takashima M, Brecht P, Torres JH, Brownell WE (2002) Membrane tether formation from outer hair cells with optical tweezers. Biophys J 82:1386–1395

Lidke DS, Lidke KA, Rieger B, Jovin TM, Arndt-Jovi DJ (2005) Reaching out for signals: filopodia sense egf and respond by directed retrograde transport of activated receptors. J Cell Biol 170:619–626

Mogilner R, Rubinstein B (2005) The physics of filopodial protrusion. Biophys J 89:782–795

Önfelt B, Nedvetzki S, Yanigi K, Davis DM (2004) Cutting edge: membrane nanotubes connect immune cells. J Immunol 173:1511–1513

Neuman KC, Block SM (2004) Optical trapping. Rev Sci Instrum 75:2787–2809

Pollard TD, Blanchoin L, Mullins RD (2000) Molecular mechanisms controlling actin filament dynamics in nonmuscle cells. Annu Rev Biophys Biomol Struct 29:545–576

Powers TR, Huber G, Goldstein RE (2002) Fluid-membrane tethers: minimal surfaces and elastic boundary layers. Phys Rev E 65:041901 1–041901 11

Ramírez-Weber F-A, Kornberg TB (1999) Cytonemes: cellular processes that project to the principal signaling center in *drosophila* imaginal discs. Cell 97:599–607

Raucher D, Sheetz MP (1999) Characteristics of a membrane reservoir buffering membrane tension. Biophys J 77:1992–2002

Rustom A, Saffrich R, Marcovik I, Walther P, Gerdes H-H (2004) Nanotubular highways for intercellular organelle transport. Science 303: 1007–1010

Rorth P (2003) Communication by touch: role of cellular extensions in complex animals. Cell 112:595–598

Sant'Anna C, Campanati L, Gadelha C, Lourenço D, Labati-Terra L, Bittencourt-Silvestre J, Benchimol M, Cunha-e-Silva NL, De Souza W (2005) Improvement on the visualization of cytoskeletal structures of protozoan parasites using high-resolution field emission scanning electron microscopy (fesem). Histochem Cell Biol 124:87–95

Schliwa M, van Blerkom J (1981) Structural interaction of cytoskeletal components. J Cell Biol 90:222–235

Sheetz MP (2001) Cell control by membrane-cytoskeleton adhesion. Nat Rev Mol Cell Biol 2:392–396

Smith A-S, Sackmann E, Seifert U (2004) Pulling tethers from adhered vesicles. Phys Rev Lett 92:28101–28104

Sun M, Graham JS, Hegedüs B, Marga F, Zhang Y, Forgacs G, Grandbois M (2005) Multiple membrane tethers probed by atomic force spectroscopy. Biophys J 89:4320–4329

Svitkina TM, Bulanova EA, Chaga OL, Vignjevic DM, Kojima S-i, Vasiliev JM, Borisy GG (2003) Mechanism of filopodia initiation by reorganization of a dendritic network. J Cell Biol 160:409–421

Titushkin I, Cho M (2006) Distinct membrane mechanical properties of human mesenchymal stem cells determined using laser optical tweezers. Biophys J 90:2582–2591

Upadhyaya A, Sheetz MP (2004) Tension in tubulovesicular networks of golgi and endoplasmic reticulum membranes. Biophys J 86:2923–2928

Viana NB, Rocha MS, Mesquita ON, Mazolli A, Maia Neto PA (2006a) Characterization of objective transmittance for optical tweezers. Appl Opt 45:4263–4269

Viana NB, Rocha MS, Mesquita ON, Mazolli A, Maia Neto PA, Nussenzveig HM (2006b) Absolute calibration of optical tweezers. Appl Phys Lett 88:131110–131113

Vignjevic D, Kojima S-, Aratyn Y, Danciu O, Svitkina T, Borisy GG (2006) Role of fascin in filopodial protrusion. J Cell Biol 174:863–875

Watkins SC, Salter RD (2005) Functional connectivity between immune cells mediated by tunneling nanotubes. Immunity 23:309–318

Wood W, Martin P (2002) Structures in focus—filopodia. Int J Biochem Cell Biol 34:726–730